Light scattering by red blood cells in ektacytometry: Fraunhofer versus anomalous diffraction

Geert J. Streekstra, Alfons G. Hoekstra, Evert-Jan Nijhof, and Robert M. Heethaar

In the present literature on ektacytometry, small angle light scattering by ellipsoidal red blood cells is commonly approximated by Fraunhofer diffraction. Calculations on a sphere with the size and relative refractive index of a red cell, however, show that Fraunhofer diffraction deviates significantly from exact Mie theory. Anomalous diffraction is found to be a much better approximation. The anomalous diffraction theory is used to calculate the intensity distribution of the light scattered by an ellipsoidally deformed red blood cell. The derived expression shows that the ellipticity of isointensity curves in forward scattered light are equal to the ellipticity of the red blood cell. The theoretical expression is fitted to the intensity patterns measured with an ektacytometer. For the small observation angles used in ektacytometry, the experimental results confirm the validity of the anomalous diffraction approach.

Key words: Anomalous diffraction, ektacytometer, ellipsoidal red blood cell, red cell deformation, isointensity curve.

Introduction

Deformability of red blood cells plays an important role in blood viscosity at shear rates exceeding 100 s^{-1} and in capillary perfusion.[1] Reduced red cell deformability causes elevation of the shear stresses on the vessel walls, which may reduce the integrity of the vessels.

In order to quantify red cell deformability, we use an ektacytometer.[2] In this apparatus cell deformability is calculated from the intensity pattern of the laser light scattered by a sheared suspension of oriented ellipsoidally deformed red blood cells. In the intensity pattern, points with equal intensity build up an elliptical isointensity curve, representing the mean ellipticity of the cell population.

Red blood cells can be considered as particles with size parameter $\alpha \gg 1$. Here α is defined as $\alpha = 2\pi R/\lambda$, where λ is the wavelength of light in the suspending medium and R is a characteristic radius of the particle. The simplest theory to approximate forward light scattering by small particles with $\alpha \gg 1$ is Fraunhofer diffraction. In this theory the intensity distribution of the scattered light is independent of the complex refractive index m of the particle relative to the surroundings. However, Mullaney and Dean[3] showed that, from a theoretical point of view, the scattering properties of biological cells (α = 70 and m = 1.05) are strongly dependent on m. Even at the small scattering angles used in ektacytometry, they found a substantial difference between Fraunhofer diffraction and the exact Mie theory.

Groner *et al.*[4] stressed the importance of optical and geometrical properties of red cells for the interpretation of scattering signals in ektacytometry. They applied the anomalous diffraction method (AM II) of Latimer *et al.*[5,6] Although the anomalous diffraction approach introduced by van de Hulst[7] seems appropriate for red blood cells ($\alpha \gg 1$ and $|m - 1| \ll 1$) there are some objections to the application of this AM II method. First, the AM II method is developed for prolate and oblate ellipsoids only. In an ektacytometer, however, the three axes of the ellipsoidal red blood cell are all different.[8] Therfore, the anomalous diffraction theory should be applied in a way that accounts for this different geometry. Second, the method of Latimer *et al.* does not directly relate the

G. J. Streekstra, E.-J. Nijhof, and R. M. Heethaar are with the Department of Medical and Physiological Physics, State University of Utrecht, University Hospital/H.02.101, P.O. Box 85500, 3508 GA Utrecht, The Netherlands. A. G. Hoekstra is with the Department of Computer Systems, Faculty of Mathematics and Computer Science, University of Amsterdam, Kruislaan 403, 1098 SJ Amsterdam, The Netherlands.

Received 18 November 1991.
0003-6935/93/132266-07$05.00/0.

cell shape to the two-dimensional intensity pattern at a certain distance from the cells.

As is shown below, anomalous diffraction applied to an oriented ellipsoidal particle gives a good approximation for small angle light scattering by red blood cells in ektacytometry and is a valuable tool for relating cell shape and size to the observed intensity pattern.

Ektacytometry

Our measuring system is slightly different from the device introduced by Bessis and Mohandas[9] and Mohandas *et al.*[10] It consists of a Contraves low shear 30 viscosimeter with an extension for deformability measurements.[2,11] A very diluted red cell suspension (0.3 vol. %) of relatively high viscosity is sheared in a Couette flow between two coaxial transparent cylinders (Fig. 1). At high shear rates, red cells deform into ellipsoids with the longest axis aligned along the streamlines.[12] A low-power He–Ne laser beam (λ = 632.8 nm) is sent through the suspension in a direction perpendicular to the streamlines. The intensity pattern of the light scattered by the red cells is projected onto a frosted glass screen and the resulting image is scanned by a video camera. The part of the intensity distribution observed by the video camera lies within a cone with an angle of approximately 10°. From the image we selected points of equal, prescribed intensity by using a microcomputer. These image points build up an elliptical curve that is related to the ellipsoidal shape of the red cell. An elliptical fit to such a curve yields a long axis l and a short axis s of the pattern.

In routine measurements, a deformation index (DI), defined by

$$\mathrm{DI} = (l - s)/(l + s), \qquad (1)$$

is measured at different angular velocities of the outer cylinder. The DI is plotted against the calculated shear stress in the suspension and represents the deformability of the red cells under consideration. It varies between 0 for undeformed circular cells to as much as a maximum value of approximately 0.5 at the highest shear stresses.

Anomalous Diffraction

The setup of the ektacytometer leads to the following assumptions concerning light scattering by ellipsoidal cells: (i) In diluted cell suspension, single and independent scattering predominates. This implicates that the intensity distribution of light scattered by an ensemble of randomly spaced particles is the sum of the distributions of the individual scatterers.[7] (ii) The intensity distribution of the incident laser beam is Gaussian. Therefore an intensity peak is superimposed on the scattered light. We assume, however, that no net phase correlation exists between this central beam and the waves of the scattered light. In consequence, the total observed intensity is the sum of the scattered light and the attenuated laser beam.

It is shown that, if anomalous diffraction is used in a form that is adapted to ellipsoids, the shape and size of the red cells in Couette flow are directly related to the spatial intensity distribution of the scattered light. Furthermore, in order to gain more insight into the applicability of anomalous diffraction to red blood cells, the influence of relative refractive index m on the light scattered by red cells is studied. The exact Mie theory is applied to a spherical model of the red cell and compared with anomalous diffraction and Fraunhofer diffraction.

Anomalous Diffraction and Red Cell Shape

In red cell suspension, the value of size parameter α is approximately 50. For this large α it is possible to distinguish between the part of the wave front that traverses and the part that passes along the particle.[7] If the light scattering is described only by the latter part, the intensity distribution is referred to as Fraunhofer diffraction. In this approximation the intensity distribution is independent of the relative refractive index m of the particle. Particles of identical cross-sectional areas therefore have identical Fraunhofer diffraction patterns. For a single ellipsoidal particle, it is possible to solve the Fraunhofer diffraction integral analytically. Consider the situation that a plane wave ψ_0 travels in the z direction of a Cartesian coordinate system (x, y, z). Let the elliptical cross-sectional area of the particle be perpendicular to the z axis and situated at the origin of this system (Fig. 2). The ellipse has a long axis $a = A\sqrt{q}$ and a short axis $b = A/\sqrt{q}$, where q denotes the ellipticity a/b and $A = \sqrt{ab}$.

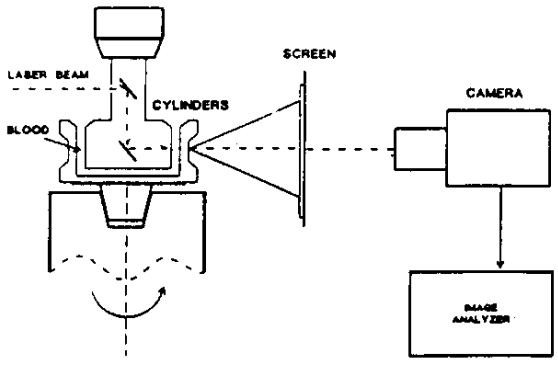

Fig. 1. Measuring configuration of the ektacytometer.

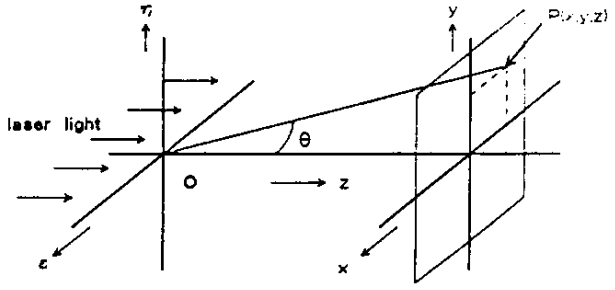

Fig. 2. Coordinate system used in the calculations of the light scattering by red blood cells in a Couette flow. The ellipsoidal red cell is situated in origin O with the longest axis directed along the ε axis. The intensity pattern is calculated in point P(x, y, z).

The intensity I_F of the diffraction part of the pattern in point P(x, y, z) is found to be (see Appendix A)

$$I_F = I_0(1/k^2r^2)|S(\nu)|^2, \quad (2)$$

with

$$S(\nu) = \alpha^2[J_1(\alpha\nu)/\alpha\nu],$$
$$r = (x^2 + y^2 + z^2)^{1/2},$$
$$\nu = \frac{1}{r}[(x^2/q) + qy^2]^{1/2},$$
$$\alpha = kA = (2\pi n_{med}/\lambda_0)A.$$

In Eq. (2) I_0 denotes the intensity of the incident wave, $J_1(u)$ is the first-order Bessel function, λ_0 is the wavelength of laser light in vacuum, and n_{med} is the refractive index of the medium that surrounds the particle. For $q = 1$, $\nu = \sin(\Theta)$ and the intensity distribution is a function of the polar angle θ only (see Fig. 2). Consequently, Eq. (2) reduces to the well-known diffraction formula for a circular cross-sectional area.[7]

In the Fraunhofer diffraction theory, only the shape and size of the cross-sectional area determine the intensity pattern. In order to account for the light that traverses the ellipsoidal cell, we used anomalous diffraction.[7] In this approach the interference between light that traverses and light that travels along the cell is considered to build up the spatial intensity distribution. Analogous to the derivation of the solution for a spherical particle, Appendix B shows that, for an ellipsoidal particle,

$$I_A = I_0(1/k^2r^2)|S(\nu)|^2, \quad (3)$$

with

$$S(\nu) = \alpha^2 \int_0^{\pi/2} [1 - \exp(-i\phi_{max} \sin\tau)] \times J_0(\alpha\nu \cos\tau)\sin\tau \cos\tau d\tau,$$
$$\phi_{max} = 2kc|m - 1|.$$

Here $J_0(u)$ denotes the zeroth-order Bessel function and c is the length of the third axis of the ellipsoid parallel to the direction of incident light. Note that, for the case of an opaque ellipsoid, the imaginary part of m is infinite and Eq. (3) correctly reduces to Eq. (2).

From Eq. (3) is is clear that all the points on the screen with a fixed value of ν build up curves of equal intensity. For $x, y \ll z$ these isointensity curve are ellipses:

$$x^2/(qz^2\nu^2) + y^2/(z^2\nu^2/q) = 1. \quad (4)$$

The ellipticity of the isointensity curves as described by Eq. (4) is equal to ellipticity q of the particle.

Assuming that Eq. (3) is suited to describe the forward scattering by oriented ellipsoidal red cells, detection of the elliptical isointensity curves immediately yields the mean ellipticity of the cell population under consideration. In this sense, by using the anomalous diffraction approximation, we can obtain quantitative information about red cell deformability.

Influence of Relative Refractive Index

In order to illustrate the influence of m, we applied the exact Mie theory to spheres with the mean radius of a red blood cell. A modified version of the Mie code[13] of Bohren and Huffman[14] was used. The results are compared to Fraunhofer [Eq. (2)] and anomalous diffraction [Eq. (3)].

Radius R of the sphere was 3.9 μm, i.e., the mean radius of a red cell population,[15] q was set to unity, and $c = R$ in Eqs. (2) and (3). With the wavelength of the He–Ne laser light and the 1.345 refractive index of the medium, the resulting value of α is 52. Since the imaginary part of m, representing the absorption of light inside the cell, is negligible,[16] m was considered to be real. In order to obtain the relation between hemoglobin concentration and the refractive index inside the cell we isolated the red cell interior.[17] The cell content was diluted with phosphate-buffered saline in order to obtain samples with different hemoglobin (Hb) concentrations. The refractive index of the samples was measured with a refractometer (Bleeker type 55007; data not shown). A second-order polynomial fit through these data yields

$$n_{int} = 1.335 + 0.001823\,\mathrm{Hb} + 8.6526 \times 10^{-6}\,\mathrm{Hb}^2. \quad (5)$$

In healthy humans the Hb concentration varies between 31.4 and 36.3 g/dL, with corresponding relative refractive indices m between 1.04 and 1.05. In pathological situations, however, the value of m might be outside this range. In our calculations m was therefore varied around the normal value, i.e., between 1.03 and 1.07. The scattering intensities are plotted as a function of polar angle θ.

Figure 3 compares Franhofer diffraction and anomalous diffraction with the exact Mie theory. The calculations clearly show that the value of m in particles with the overall size of the red blood cell appear to be important for intensity distribution.

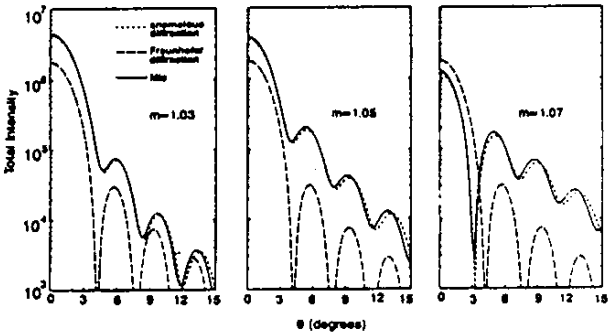

Fig. 3. Comparison of anomalous diffraction, Fraunhofer diffraction, and the Mie theory for a spherical model of the red blood cell (R = 3.9 μm, α = 52).

In contradiction to Fraunhofer diffraction, anomalous diffraction agrees well with the exact Mie theory within the angle of 10° in which we are interested. The agreement between Mie theory and anomalous diffraction is the best for the lowest value of m. When m increases, the maximum intensity at $\Theta = 0$ decreases as a consequence of destructive interference between the light that traverses and travels along the sphere. The first minimum of the intensity pattern is shifted toward a significantly smaller angle for $m = 1.07$. These phenomena are well described by anomalous diffraction but are totally absent in Fraunhofer diffraction.

Experiments

In order to investigate the applicability of the anomalous diffraction in practice, we investigated the intensity pattern caused by a suspension of sheared red blood cells.

Polyvinylpyrrolidone (7 wt. %) was dissolved in a phosphate-buffered saline solution, (290 mOsm/L, pH 7.4), in order to obtain a high medium viscosity of 60 mP. Anticoagulated whole blood of a healthy donor was added to the medium that was preheated at 37 °C just before measurement. The red cell concentration was 0.3 vol. %.

Two different shear stresses (0.18 and 2.1 N/m²) were applied to obtain two values of ellipticity q. At both shear rates, ten images were scanned. The mean of the images was calculated, representing the time average of the intensity pattern on the screen. Isointensity curves as well as the angular dependency of the normalized intensity pattern are presented in Fig. 4.

At the lowest shear rate the cells are not significantly deformed and will be either directed along the streamlines or randomly oriented. The corresponding intensity pattern is nearly circular (Fig. 4, left panel). Two theoretical curves, which were obtained by using both Fraunhofer diffraction [Eq. (2)] and anomalous diffraction [Eq. (3)], are calculated and plotted through the measured intensity distribution. The polar angle θ is in the plane $y = 0$ (see Fig. 2). In the calculation, parameters of the average spherical red blood cell[15] are substituted directly into Eqs. (2) and (3), i.e., $\alpha = 52$, $m = 1.05$, and $q = 1$. Note that for angles smaller than approximately 3° the normalized intensity patterns calculated by Fraunhofer diffraction and anomalous diffraction coincide.

Increasing the shear rate to 2.1 N/m² results in a pattern that corresponds to a value of $q > 1$ (Fig. 4, right panel). The polar angle Θ is in the planes $y = 0$ and $x = 0$ for the short and long axes of the pattern, respectively. Equations (2) and (3) are used to fit the theoretical curves through the measurements. For the calculation of these curves we must obtain the parameters α, q, and c. From the isointensity curve q turned out to be 2.34. The values of α that resulted in a proper fit to the measured data were 47 and 53 for Fraunhofer diffraction and anomalous diffraction, respectively. The third axis c that corresponds to this α is calculated from $c = 3\pi V(n_{med}/\lambda_0\alpha)^2$, where V is the mean volume of the red blood cell population ($V = 90$ fL).[15] For Fraunhofer diffraction c was 1.72 μm and for anomalous diffraction c was 1.36 μm. The relative refractive index m was set at 1.05 again in Eq. (3). At this higher shear stress Fraunhofer diffraction and anomalous diffraction co-

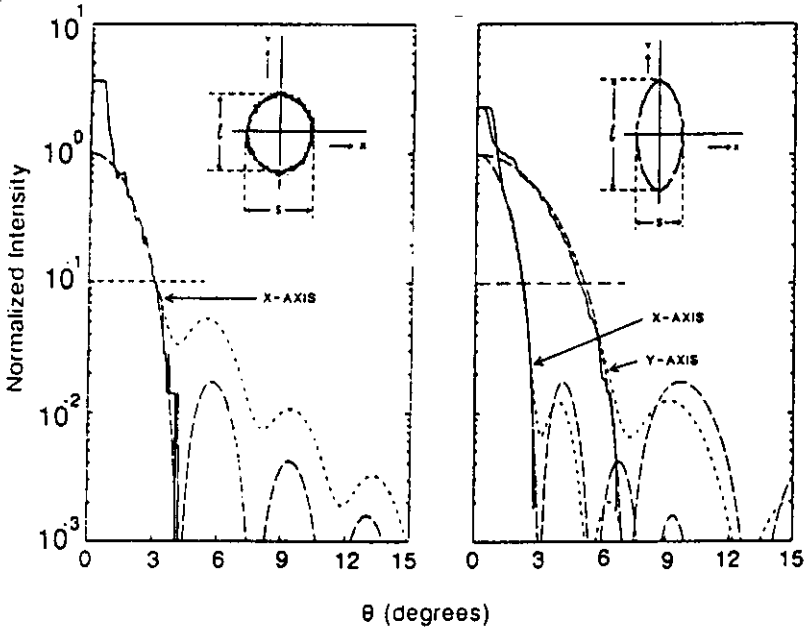

Fig. 4. Normalized intensity patterns and the isointensity curves (insets) at shear stresses of 0.18 N/m² (left panel) and 2.1 N/m² (right panel). The solid curves represent the measurements and the dashed curves represent the theoretical curves (– – – –, anomalous diffraction; —— ——, Fraunhofer diffraction). The theoretical curves were normalized by setting the scattering intensity at zero degrees to unity. The experimental curves were shifted to obtain optimal agreement with the theoretical curves.

incide at small angles only for different values of size parameter α. Although ellipticity q is equal in the application of both theories (since q is related to the isointensity curves in the same way) the difference in α results in different absolute values of a, b, and c.

At angles Θ smaller than approximately 2°, the central laser beam significantly elevates the intensity pattern above the theoretical curves. At large Θ, the measured intensity pattern starts to deviate from both Fraunhofer and anomalous diffraction just before the first local minimum in the calculated curves. The isointensity curves should therefore be scanned at angles $\Theta > 2°$, but within the first minimum of the theoretical curve.

Discussion

In the literature on ektacytometry[2,9,10,18,19] the mechanism of forward light scattering by red cells is assumed to be Fraunhofer diffraction. From the calculations shown in Fig. 3 it is clear that, for the case of a sphere with radius and relative refractive index m of the red cell, Fraunhofer diffraction deviates significantly from the exact Mie theory. The anomalous diffraction approach, however, eliminates the main part of this deviation by adding the light that traverses the particle to the diffracted light. Figure 3 shows a good agreement of anomalous diffraction with the exact theory for the spherical model of the red blood cell.

Although red cells are not spheres under flow conditions, Fraunhofer diffraction [Eq. (2)] will also deviate from the exact solution for ellipsoids. Therefore a better theory is needed to describe the light scattering of the ellipsoidal red blood cells. For that purpose the T-matrix method developed by Barber *et al.*[20] is available. For ellipsoids, however, the advantage of anomalous diffraction compared to this exact theory is the straightforward interpretation of the intensity pattern. In the case of a suspension of equally deformed ellipsoidal red blood cells the ellipticity of the red cells is equal to the ellipticity of the isointensity curves in the intensity pattern. Furthermore, apart from q, the mean values of α and c are easily obtained by fitting Eq. (3) to the measurements.

The measurements at the highest shear stress (Fig. 4, right panel) illustrate the discrepancy between Fraunhofer diffraction and anomalous diffraction for ellipsoidal cells. Although both Fraunhofer diffraction and anomalous diffraction fit the measurements to within the first minimum of the intensity pattern the values of α and c are different. In anomalous diffraction, however, the light transmitted by the cell is taken into account and therefore the results obtained by using this theory are more accurate. The agreement of anomalous diffraction with the exact theory in a spherical model of the red blood cell supports this thesis.

The direct relationship between red cell shape and the observed intensity pattern is limited to the cases in which the cells are aligned parallel to the direction of the flow and have uniform deformation. Considering a normal population of ellipsoidally deformed red blood cells there will always be a distribution in the parameters α and m, the ellipticity q, and in the third axis c of the ellipsoid. As a consequence the resulting ellipticity of the intensity pattern may deviate from the statistical average of the ellipticities of the cells in the population.

From a rheological point of view it is important to have a method to obtain the three axes of the ellipsoidal red blood cell. By usng the numerical values of a, b, and c it is possible to calculate mean values of the rheological parameters of the red cell membrane, i.e., the surface shear viscosity (η_m) and the shear elasticity modulus (μ_m).[21–23] These parameters are the determining factors for the dynamic behavior of red blood cells in the circulation and are therefore better indicators for hematological diseases than ellipticity q or the deformation index, $DI = (q - 1)/(q + 1)$. Another advantage of the deduction of membrane parameters from a, b, and c is that the results can be compared to other techniques such as the micropipette technique and rheoscopy for which the results are also expressed in terms of membrane parameters. Although in ektacytometry it is possible to obtain only mean values of the membrane parameters, the advantage compared to rheoscopy and the micropipette technique is its suitability for routine measurements in clinical studies.

The procedure to obtain mean values of a, b, and c as described here is applicable only for the cases that the cells are steadily tank treading. However, in hemolytic anemias such as hereditary spherocytosis and sickle cell disease, patients have a subpopulation of undeformable red blood cells that are not aligned along the streamlines of the flow. In an ektacytometer these cells rotate around an axis perpendicular to the streamlines of the flow.[24,25] Consequently, an additional intensity pattern is superimposed on the elliptical pattern caused by the normal ellipsoidal red blood cells. This pattern is circular or elliptical with the longest axis perpendicular to the longest axis of the normal pattern. The resulting composite intensity pattern appears to deviate significantly from the elliptical pattern observed in a normal red cell population. In order to account for the additional component in the pattern we can apply anomalous diffraction to the rotating and differently shaped subpopulation of undeformable red blood cells. Adding this component to the intensity pattern of the ellipsoidally deformed red blood cells, taking into account the ratio of deformable and undeformable red blood cells, we can calculate the total intensity pattern. The resulting theoretical intensity pattern can be fit to the measurement with the ratio of deformable and undeformable cells as a parameter.

In order to check the accuracy of the anomalous diffraction theory for ellipsoidal red blood cells, the next step that must be taken in future research is a comparison of the results obtained by Eq. (3) to the existing exact theory.[20] In future experimental work,

rheoscopic measurements[26] will be performed in order to quantify the distributions of α, q, and c in a red cell population. These data will be used to investigate the effect of these distributions on the shape of the isointensity curves and the calculation of the mean values of a, b, and c.

Conclusions

The anomalous diffraction, in the way presented in this paper, gives a good insight into the light scattering by red blood cells in ektacytometry. In particular, the relation between cell shape and intensity pattern is immediately evident in this approximation. The calculations for spheres show that, in contradiction to Fraunhofer diffraction, anomalous diffraction gives a correct description of the light scattering by particles with size parameter ($\alpha = 52$) and refractive index ($m = 1.05$) of the red blood cell. These findings will be useful for the interpretation of the deformability measurements with an ektacytometer and for the determination of membrane parameters of a red cell population.

The authors thank P. M. A. Sloot, University of Amsterdam, for careful reading of the manuscript and for valuable suggestions and J. J. Sixma, University of Utrecht, for his support concerning the hematological aspects of this research.

This work was supported by the Dutch Ministry of Economic Affairs, Sondag Optische Instrumenten B. V., and The Netherlands Organization for Scientific Research, grant NWO 810-410-041.

Appendix A: Fraunhofer Diffraction

The theory describing the intensity distribution in the forward direction of a uniformly illuminated opaque particle is called Fraunhofer diffraction. Consider an arbitrary opaque particle situated in the origin of a Cartesian coordinate system (ε, η, z) illuminated by a plane wave that travels in the z direction (Fig. 2). The intensity at point $P(x, y, z)$ at a distance that is large compared to the dimensions of the particle is given by[7]

$$I = I_0 \frac{|S(\beta, \gamma)|^2}{k^2 r^2} \tag{A1}$$

with

$$r = (x^2 + y^2 + z^2)^{1/2}, \tag{A2}$$

$$\beta = x/r, \qquad \gamma = y/r. \tag{A3}$$

I_0 denotes the intensity of the incident beam and k is the value of the wave vector in the medium that surrounds the particle. The amplitude function $S(\beta, \gamma)$ is obtained by calculating the diffraction integral:

$$S(\beta, \gamma) = (k^2/2\pi) \iint_{A_{sc}} \exp[-ik(\varepsilon\beta + \eta\gamma)]\mathrm{d}\varepsilon\mathrm{d}\eta. \tag{A4}$$

In Eq. (A4) the integral is taken over the cross-sectional area, A_{sc}, of the particle in the plane defined by $z = 0$.

In the case of an ellipsoid with principal axes a, b, and c in the ε, η, and z directions, respectively, the cross-sectional area is an ellipse with principal axes a and b. It is useful to transform the coordinates of that area (ε, η, z) to (ρ, δ, z) and those of the observer point $P(x, y, z)$ to (ν, φ, z):

$$\varepsilon = (\rho/\sqrt{q})\cos\delta, \qquad \beta = (\nu\sqrt{q})\cos\varphi,$$

$$\eta = (\rho\sqrt{q})\sin\delta, \qquad \gamma = (\nu\sqrt{q})\sin\varphi, \tag{A5}$$

where q is the ellipticity a/b of the elliptical cross-sectional area A_{sc}.

Substituting Eqs. (A5) into Eq. (A4), the explicit form of the diffraction integral for an ellipsoidal particle becomes

$$S(\nu, \varphi) = (k^2/2\pi) \int_0^A \left| \int_0^{2\pi} \exp[-ik\rho\nu\cos(\varphi - \delta)]\mathrm{d}\delta \right| \rho\mathrm{d}\rho,$$

where $A = \sqrt{ab}$. The integral over δ is performed by using the integral form of the zeroth-order Bessel function:

$$J_0(\mu) = (1/2\pi) \int_0^{2\pi} \exp[-i\mu\cos(\delta)]\mathrm{d}\delta, \tag{A7}$$

with a resulting $S(\nu, \varphi)$ that is not dependent on φ:

$$S(\nu) = k^2 \int_0^A J_0(k\nu\rho)\rho\mathrm{d}\rho.$$

By using $\mu J_0 = d(\mu J_1)/\mathrm{d}\mu$, we finally found $S(\nu)$ to be

$$S(\nu) = \alpha^2[J_1(\alpha\nu)/\alpha\nu], \tag{A9}$$

where the size parameter $\alpha = kA$ and $J_1(u)$ is the first-order Bessel function of u.

Appendix B: Anomalous Diffraction

In the anomalous diffraction approach the light that traverses the particle is taken into account.[7] This light is phase shifted compared to the Fraunhofer light that travels along the particle. Interference of the phase-shifted light with the Fraunhofer light determines the spatial intensity distribution. The validity of the anomalous diffraction theory is restricted to values of m near 1 (minor deflection and reflection of the light at the medium–particle interface) and large values of an overall size parameter α.

Applying the Huygens' principle to a plane just behind the particle, the integrand in the expression for the amplitude function [Eq. (A4)] gets an addi-

tional term that involves the phase shift $\phi(\varepsilon, \eta)$:

$$S(\beta, \gamma) = (k^2/2\pi) \iint_{A_{sc}} \{1 - \exp[-i\phi(\varepsilon, \eta)]\} \times \exp[ik(\varepsilon\alpha + \eta\gamma)]d\varepsilon d\eta. \quad \text{(A10)}$$

By considering an ellipsoidal particle as described in Appendix A, we found $\phi(\varepsilon, \eta)$ to be

$$\phi(\varepsilon, \eta) = 2kc|m - 1|[1 - (\varepsilon^2/a^2) - (\eta^2/b^2)]^{1/2}. \quad \text{(A11)}$$

Performing the coordinate transformation Eqs. (A5) and applying Eq. (A7) results in the expression for $S(\nu)$:

$$S(\nu) = k^2 \int_0^A \{1 - \exp[-i\phi(\rho)]\} J_0(k\nu\rho)\rho d\rho, \quad \text{(A12)}$$

where $\phi(\rho) = 2kc|m - 1|[1 - (\rho^2/A^2)]^{1/2}$. By using, in analogy to the derivation of van de Hulst for spheres,[7] the substitutions $\rho = A \cos \tau$ and $\phi_{max} = 2kc|m - 1|$, $S(\nu)$ is finally given by

$$S(\nu) = \alpha^2 \int_0^{\pi/2} \{1 - \exp[-i\phi_{max} \sin(\tau)]\} \times J_0(\alpha\nu \cos \tau)\sin \tau \cos \tau d\tau. \quad \text{(A13)}$$

References

1. S. Chien, J. Dormandy, E. Ernst, and A. Matrai, *Clinical Hemorheology* (Nijhoff, Boston, Mass., 1987), Chap. 5, p. 129.
2. J. H. F. I. van Breugel, "Hemorheology and its role in blood platelet adhesion under flow conditions," Ph.D. dissertation (State University of Utrecht, Utrecht, The Netherlands, 1989).
3. P. F. Mullaney and P. N. Dean, "The small angle light scattering of biological cells," Biophys. J. **10**, 764–772 (1970).
4. W. Groner, N. Mohandas, and M. Bessis, "New optical technique for measuring erythrocyte deformability with the ektacytometer," Clin. Chem. **26**, 1435–1442 (1980).
5. P. Latimer, "Light scattering by ellipsoids," J. Colloid Interface Sci. **53**, 102–109 (1975).
6. P. Latimer and P. Barber, "Scattering by ellipsoids of revolution," J. Colloid Interface Sci. **63**, 310–316 (1978).
7. H. C. van de Hulst, *Light Scattering by Small Particles* (Wiley, New York, 1957), Chap. 11, p. 183.
8. S. R. Keller and R. Skalak, "Motion of a tank-treading ellipsoidal particle in a shear flow," J. Fluid Mech. **120**, 27–47 (1982).
9. M. Bessis and N. Mohandas, "A diffractometric method for the measurement of cellular deformability," Blood Cells **1**, 307–313 (1975).
10. N. Mohandas, M. R. Clark, M. S. Jacobs, and S. B. Shohet, "Analysis of factors regulating erythrocyte deformability," J. Clin. Invest. **66**, 563–573 (1980).
11. M. R. Hardeman, P. Goedhart, and D. Breederveld, "Laser diffraction ellipsometry of erythrocytes under controlled shear stress using a rotational viscosimeter," Clin. Chim. Acta **165**, 227–234 (1987).
12. T. Fischer and H. Schmidt-Schönbein, "Tank tread motion of red cell membranes in viscometric flow: behavior of intracellular and extracellular markers (with film)," Blood Cells **3**, 351–365 (1977).
13. P. M. A. Sloot, A. G. Hoekstra, H. v. d. Liet, and C. G. Figdor, "Scattering matrix elements of biological particles measured in a flow through system: theory and practice," Appl. Opt. **28**, 1752–1762 (1989).
14. C. F. Bohren, D. R. Huffman, *Absorption and Scattering of Light by Small Particles* (Wiley, New York, 1957), App. A, p. 479.
15. Y. C. Fung, *Biomechanics*, 2nd ed. (Springer-Verlag, New York, 1984), Chap. 4, p. 106.
16. L. Reynolds, C. Johnson, and A. Ishimaru, "Diffuse reflectance from a finite blood medium: applications to the modeling of fiber optic catheters," Appl. Opt. **15**, 2059–2067 (1976).
17. G. R. Cokelet and H. J. Meiselman, "Rheological comparison of hemoglobin solutions and erythrocyte suspensions," Science **162**, 275–277 (1968).
18. J. Plazek and T. Marik, "Determination of undeformable erythrocytes in blood samples using laser light scattering," Appl. Opt. **21**, 4335–4338 (1982).
19. F. Storzicky, V. Blazek, and J. Muzik, "An improved diffractometric method for measurement of cellular deformability," J. Biomech. **13**, 417–421 (1980).
20. P. Barber and C. Yeh, "Scattering of electromagnetic waves by arbitrarily shaped dielectric bodies," Appl. Opt. **14**, 2864–2872 (1975).
21. R. Tran-Son-Tay, S. P. Sutera, and P. R. Rao, "Determination of red blood cell membrane viscosity from rheoscopic observations of tank-treading motion," Biophys. J. **46**, 65–72 (1984).
22. R. Tran-Son-Tay, S. P. Sutera, G. I. Zahalak, and P. R. Rao, "Membrane stress and internal pressure in a red blood cell freely suspended in a shear flow," Biophys. J. **51**, 915–924 (1987).
23. S. P. Sutera, P. R. Pierre, and G. I. Zahalak, "Deduction of intrinsic mechanical properties of the erythrocyte membrane from observations of tank-treading in the rheoscope," Biorheology **26**, 177–197 (1989).
24. C. Allard, N. Mohandas, and M. Bessis, "Red cell deformability changes in hemolytic anemias estimated by diffractometric methods (ektacytometry)," Blood Cells **3**, 209–221 (1977).
25. M. Bessis and N. Mohandas, "Laser diffraction patterns of sickle cells in fluid shear fields," Blood Cells **3**, 229–239 (1977).
26. G. J. Streekstra, E.-J. Nijhof, and R. M. Heethaar, "A bi-plane rheoscope: a new approach in optical determination of red blood cell orientation and deformation in a Couette flow," in *Proceedings of the North Sea Conference on Biomedical Engineering*, J. Cornelis and S. Peters, eds. (International Federation for Medical and Biological Engineering, Antwerp, 1990).